

# Final-state $NN$ -rescattering in spin asymmetries of $d(\gamma, \pi^-)pp$ reaction

Eed M. Darwish \*

*Physics Department, Faculty of Science, South Valley University,  
Sohag 82524, Egypt*

Agus Salam

*Departemen Fisika, FMIPA, Universitas Indonesia, Depok 16424, Indonesia*

---

## Abstract

The role of the final-state  $NN$ -rescattering ( $NN$ -FSI) in the polarization observables of the inclusive reaction  $d(\gamma, \pi^-)pp$ , involving polarization of the photon beam and/or the deuteron target, is investigated. Various single- and double-spin asymmetries are studied with respect to the influence of such interaction effect and numerical predictions are given for forthcoming experiments. It has been found that the effect of  $NN$ -FSI is quite important for the single-spin asymmetries  $\Sigma$ ,  $T_{20}$ ,  $T_{21}$  and  $T_{22}$  and the double-spin asymmetry  $T_{20}^\ell$ , whereas it is much less important for the vector target asymmetry  $T_{11}$  and other beam-target double-polarization asymmetries. Furthermore, we found that the inclusion of the  $NN$ -FSI improves the description of the LEGS data for the linear photon asymmetry.

*PACS:* 24.70.+s; 14.20.-c; 13.60.Le; 25.20.Lj; 25.20.-x; 25.30.Fj

*Keywords:* Polarization phenomena in reactions; Spin observables; Meson production; Photoproduction reactions; Photonuclear reactions; Final-state interactions.

---

## 1 Introduction and Motivation

A still very interesting topic in medium-energy nuclear physics is concerned with the role of effective degrees of freedom in hadronic systems in terms of nucleons, mesons and isobars. In particular, the connection of such effective degrees of freedom to the underlying quark-gluon dynamics of Quantum

---

\* Corresponding author.

*Electronic address:* eeddarwish@yahoo.com (E.M. Darwish).

Chromodynamics (QCD) has still to be clarified. For the study of these basic questions, the two-nucleon system provides an important test laboratory. First of all, it is the simplest nuclear system for the study of the  $NN$  interaction. Moreover, due to the lack of free neutron targets, the deuteron is the simplest nucleus which can be used to extract neutron properties.

Interest in pion photoproduction from light nuclei has increased mainly through the construction of new high-duty continuous electron beam machines such as MAMI in Mainz, ELSA in Bonn, LEGS in Brookhaven or JLab in Newport News (for an experimental overview see [1,2]). In conjunction with these experimental efforts, we investigate in this work the reaction  $d(\gamma, \pi^-)pp$  including final-state interaction (FSI) effects with special emphasis on polarization observables. Spin physics proves to be a vital element and indispensable tool in our venture of revealing the internal structure of hadronic matter. It is a well-known fact that in order to study further details of a reaction one has to study polarization observables like, e.g., beam asymmetry, target asymmetries and beam-target asymmetries. These additional observables contain interference terms of the various amplitudes in different combinations from which one can determine all amplitudes provided one has measured a complete set of observables.

Up to present times, most of calculations for incoherent pion photoproduction from the deuteron have considered only the unpolarized observables like differential and total cross sections [3,4,5,6,7,8,9,10,11]. Notwithstanding this continuing effort to study this process, the wealth of information contained in it has not yet been fully exploited. Since the  $t$ -matrix has 12 independent complex amplitudes, one has to measure 23 independent observables, in particular, in order to determine completely the  $t$ -matrix. The unpolarized differential and total cross sections provide information only on the sum of the absolute squares of the amplitudes, whereas polarization degrees of freedom lead to new observables which provide additional information on the nuclear structure as well as on the reaction mechanism.

Polarization observables for incoherent pion photoproduction on the deuteron with polarized photon beam and/or polarized deuteron target have been poorly investigated. The influence of  $NN$ - and  $\pi N$ -rescattering on the analyzing powers in the quasifree  $\pi^-$ -photoproduction reaction on the deuteron in the  $\Delta$ -resonance region has been studied within a diagrammatic approach [12] using relativistic-invariant forms of the photoproduction and  $\pi N$  scattering operators. In that work, calculations for analyzing powers connected to beam and target polarization, and to polarization of one of the final protons are given. It has been shown that the effects of rescattering play a noticeable role in the behaviour of these observables in the kinematic region of the  $\Delta$ -isobar with large momenta of protons in the final state. The deuteron tensor analyzing power components in negative pion photoproduction from the deuteron have

been studied in the pure impulse approximation (IA) [13] using deuteron wave function of different realistic potential models. It was shown that the influence of rescattering effects is necessary and must be taken into account in the analysis of experimental data. In our previous evaluation [14], special emphasizes are given for the beam-target spin asymmetry of the total cross section and the Gerasimov-Drell-Hearn (GDH) sum rule for the deuteron including  $NN$ - and  $\pi N$ -rescattering in the final state. We found that FSI reduce the value of the GDH integral to about half of the value obtained for the pure IA.

Various single- and double-polarization asymmetries of the differential cross section in incoherent pion photoproduction from the deuteron have been discussed in our recent papers [15,16,17] without any kind of FSI effects. The sensitivity of these spin observables to the model deuteron wave function has been investigated. We found that interference of Born terms and the  $\Delta(1232)$ -contribution plays a significant role. Furthermore, our results for the linear photon asymmetry [17,18] have been compared with the preliminary experimental data from the LEGS Spin collaboration [19] and major discrepancies were evident. Since a strong influence of the FSI on the unpolarized cross sections was found in [10], one might expect that the LEGS data can be understood in terms of the FSI and possibly two-body effects. It has been found in [18], that  $NN$ -FSI is quite important and leads to a better agreement with existing experimental data. Moreover, we have investigated most recently the influence of final-state  $NN$ -rescattering on the helicity structure of the  $\vec{\gamma}\vec{d} \rightarrow \pi^- pp$  reaction [20,21]. The differential polarized cross-section difference for the parallel and antiparallel helicity states has been predicted and compared with recent experimental data from MAMI (Mainz/Pavia) [22]. It has been shown that the effect of  $NN$ -rescattering is much less important in the polarized differential cross-section difference than in the unpolarized one.

As a further step in this direction, we investigate in this paper the role of the  $NN$ -rescattering effect in several single- and double-polarization observables of photon and deuteron target in negative pion photoproduction from the deuteron with polarized photon beam and/or oriented deuteron target. The understanding of this mechanism is of great importance to understand the basic  $NN$  interaction. The  $\pi N$ -rescattering contribution is found to be negligible [9,10] and thus it is not considered in the present work. The second point of interest is to analyze the preliminary experimental data for the linear photon asymmetry  $\Sigma$  from LEGS [19] in order to keep up with the development of the experimental side.

The structure of this paper is as follows. In Sect. 2, the model for the elementary  $\gamma N \rightarrow \pi N$  and  $NN \rightarrow NN$  reactions which will serve as an input for our calculation of the reaction on the deuteron is briefly summarized. In Sect. 3 we provide some details about the reaction on the deuteron. The general formalism and the separate contributions of the pure IA and the  $NN$ -FSI to the

transition matrix, based on time-ordered perturbation theory, are described in this section. The formal expressions for various polarization observables in terms of the transition amplitude are given in Sect. 4. Details of the actual calculations and the results for the pure IA as well as for the inclusion of the FSI in the  $NN$  system are presented and discussed in Sect. 5. Finally, a summary and conclusions are given in Sect. 6.

## 2 Elementary reactions

Incoherent pion photoproduction from the deuteron is governed by basic two-body processes, namely pion photoproduction on a nucleon and hadronic two-body scattering reactions. For the latter only  $NN$  scattering in the two-body subsystems is considered in this work. In the following, we will briefly summarize these two elementary processes, i.e., the  $\gamma N \rightarrow \pi N$  and  $NN \rightarrow NN$  reactions.

### 2.1 The $\gamma N \rightarrow \pi N$ process

The starting point of the construction of an operator for pion photoproduction on the two-nucleon space is the elementary pion photoproduction operator on a single nucleon, i.e.,  $\gamma N \rightarrow \pi N$ . In the present work we will examine the various observables for the reaction on the nucleon using, as in our previous work [10], the effective Lagrangian model developed by Schmidt *et al.* [8]. The main advantage of this model is that it has been constructed in an arbitrary frame of reference and allows a well defined off-shell continuation as required for studying pion production on nuclei. It consists of the standard pseudovector Born terms and the contribution of the  $\Delta(1232)$ -resonance. For further details with respect to the elementary pion photoproduction operator we refer to [8]. As shown in Figs. 1-3 in our previous work [10], the results of our calculations for the elementary process are in good agreement with recent experimental data as well as with other theoretical predictions and gave a clear indication that this elementary operator is quite satisfactory for our purpose, namely to incorporate it into the reaction on the deuteron.

### 2.2 Nucleon-nucleon scattering

For the nucleon-nucleon scattering in the  $NN$ -subsystem we use in this work a specific class of separable potentials [23] which historically have played and still play a major role in the development of few-body physics and also fit the phase

shift data for  $NN$ -scattering. The EST method [24] for constructing separable representations of modern  $NN$  potentials has been applied by the Graz group [23] to cast the Paris potential [25] in separable form. This separable model is most widely used in case of the  $\pi NN$  system (see for example [26] and references therein). Therefore, for the present study of the influence of  $NN$ -rescattering this model is good enough.

### 3 The $\gamma d \rightarrow \pi NN$ reaction

Following the formulation of our previous work [10], the general form for the unpolarized cross section in incoherent pion photoproduction from the deuteron is given according to [27] by

$$d\sigma = \frac{\delta^4(k + d - p_1 - p_2 - q) M_N^2 d^3 p_1 d^3 p_2 d^3 q}{96(2\pi)^5 |\vec{v}_\gamma - \vec{v}_d| \omega_\gamma E_d E_1 E_2 \omega_q} \times \sum_{smt} \sum_{m_\gamma m_d} \left| \mathcal{M}_{smm_\gamma m_d}^{(t\mu)}(\vec{p}_1, \vec{p}_2, \vec{q}, \vec{k}, \vec{d}) \right|^2, \quad (1)$$

The semi-inclusive unpolarized differential cross section, where only the final pion is detected without analyzing its energy, is given from (1) by

$$\frac{d\sigma}{d\Omega_\pi} = \frac{1}{6} \int_0^{q_{max}} dq \iint d\Omega_{p_{NN}} \rho_s \sum_{smt} \sum_{m_\gamma m_d} \left| \mathcal{M}_{smm_\gamma m_d}^{(t\mu)}(\vec{p}_{NN}, \vec{q}, \vec{k}) \right|^2. \quad (2)$$

The transition  $\mathcal{M}$ -matrix elements are calculated in the frame of time-ordered perturbation theory, using the elementary pion photoproduction operator introduced in section 2 and including  $NN$ -rescattering in the final state. The amplitude of the  $\gamma d \rightarrow \pi NN$  reaction is determined by the transition matrix

$$\mathcal{M}_{smm_\gamma m_d}^{(t\mu)}(\vec{k}, \vec{q}, \vec{p}_1, \vec{p}_2) = {}^{(-)}\langle \vec{q} \mu, \vec{p}_1 \vec{p}_2 s m t - \mu | \epsilon_\mu(m_\gamma) J^\mu(0) | \vec{d} m_d 00 \rangle, \quad (3)$$

where  $J^\mu(0)$  denotes the current operator. In principle, the full treatment of all interaction effects requires a three-body treatment. However, the outgoing  $\pi NN$  scattering state is approximated in this work by

$$|\vec{q} \mu, \vec{p}_1 \vec{p}_2 s m t - \mu\rangle^{(-)} = |\vec{q} \mu, \vec{p}_1 \vec{p}_2 s m t - \mu\rangle + \hat{G}_0^{\pi NN(-)} \hat{T}^{NN} |\vec{q} \mu, \vec{p}_1 \vec{p}_2 s m t - \mu\rangle, \quad (4)$$

where  $|\vec{q} \mu, \vec{p}_1 \vec{p}_2 s m t - \mu\rangle$  denotes the free  $\pi NN$  plane wave,  $\hat{G}_0^{\pi NN(-)}$  the

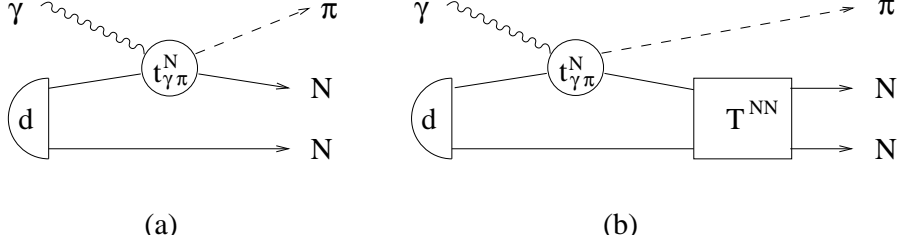


Figure 1. Diagrammatic representation of incoherent pion photoproduction from the deuteron including  $NN$ -rescattering in the final state: (a) impulse approximation (IA) and (b)  $NN$ -rescattering.

free  $\pi NN$  propagator and  $\hat{T}^{NN}$  the reaction operator for  $NN$ -scattering. In this approximation, the total transition matrix element reads

$$\mathcal{M}_{s m m_\gamma m_d}^{(t\mu)} = \mathcal{M}_{s m m_\gamma m_d}^{(t\mu) IA} + \mathcal{M}_{s m m_\gamma m_d}^{(t\mu) NN}, \quad (5)$$

where the first term denotes the transition matrix of the pure IA which means that the reaction will take place only on one of the nucleons leaving the other as a pure spectator (see diagram (a) in Fig. 1). The second term represents the corresponding matrix for the  $NN$ -rescattering (see Fig. 1(b)).

Denoting the matrix element of the elementary production on a nucleon by  $\hat{t}_{\gamma\pi}^N$ , the amplitude of the IA-term in the deuteron lab-frame reads [10]

$$\mathcal{M}_{s m m_\gamma m_d}^{(t\mu) IA}(\vec{k}, \vec{q}, \vec{p}_1, \vec{p}_2) = \sqrt{2} \sum_{m'} \langle s m, t - \mu | \left( \langle \vec{p}_1 | \hat{t}_{\gamma\pi}^N(\vec{k}, \vec{q}) | -\vec{p}_2 \rangle \tilde{\Psi}_{m', m_d}(\vec{p}_2) - (-)^{s+t} (\vec{p}_1 \leftrightarrow \vec{p}_2) \right) | 1 m', 00 \rangle, \quad (6)$$

where  $|1 m', 00\rangle$  denotes the two-nucleon spin and isospin wave function.

By using the information in Ref. [10], we can write the  $NN$ -rescattering term in (5) as

$$\mathcal{M}_{s m m_\gamma m_d}^{(t\mu) NN}(\vec{k}, \vec{q}, \vec{p}_1, \vec{p}_2) = \sum_{m'} \iiint d^3 \vec{p}'_{NN} \sqrt{\frac{E_1 E_2}{E'_1 E'_2}} \tilde{\mathcal{R}}_{s m m'}^{NN, t\mu}(W_{NN}, \vec{p}_{NN}, \vec{p}'_{NN}) \times \frac{M_N}{\tilde{p}^2 - p'^2_{NN} + i\epsilon} \mathcal{M}_{s m', m_\gamma m_d}^{(t\mu) IA}(\vec{k}, \vec{q}, \vec{p}'_1, \vec{p}'_2). \quad (7)$$

The conventional  $NN$ -scattering matrix  $\tilde{\mathcal{R}}_{s m m'}^{NN, t\mu}$  is introduced with respect to noncovariantly normalized states. It is expanded in terms of the partial wave contributions  $\mathcal{T}_{J s \ell \ell'}^{NN, t\mu}$  as follows

$$\begin{aligned}\widetilde{\mathcal{R}}_{smm'}^{NN,t\mu}(W_{NN},\vec{p}_{NN},\vec{p}'_{NN}) &= \sum_J \sum_{\ell\ell'} \mathcal{F}_{\ell\ell'mm'}^{NN,J_s}(\hat{p}_{NN},\hat{p}'_{NN}) \\ &\times \mathcal{T}_{Js\ell\ell'}^{NN,t\mu}(W_{NN},p_{NN},p'_{NN}),\end{aligned}\quad (8)$$

where the purely angular function  $\mathcal{F}_{\ell\ell'mm'}^{NN,J_s}(\hat{p}_{NN},\hat{p}'_{NN})$  is defined by

$$\mathcal{F}_{\ell\ell'mm'}^{NN,J_s}(\hat{p}_{NN},\hat{p}'_{NN}) = \sum_M \sum_{m_\ell m_{\ell'}} C_{m_\ell m_M}^{\ell s J} C_{m_{\ell'} m'_M}^{\ell' s J} Y_{\ell m_\ell}^*(\hat{p}_{NN}) Y_{\ell' m_{\ell'}}(\hat{p}'_{NN}). \quad (9)$$

The necessary half-off-shell  $NN$ -scattering matrix  $\mathcal{T}_{Js\ell\ell'}^{NN,t\mu}$  was obtained from separable representation of a realistic  $NN$ -interaction [23]. Explicitly, all  $S$ ,  $P$ , and  $D$  waves were included in the  $NN$ -scattering matrix.

#### 4 Polarization observables

Since calculational details associated with the evaluation of the polarization observables in incoherent pion photoproduction from the deuteron were considered in our previous papers [15,17] there is no need to repeat them here. However, we briefly recall the necessary definitions of observables.

In the present work, we consider the following polarization observables:

(i) The linear photon asymmetry

$$\Sigma = \frac{2}{\mathcal{Q}} \mathcal{R}e \sum_{smt} \sum_{m_d} \int_0^{q_{\max}} dq \iint d\Omega_{p_{NN}} \rho_s \mathcal{M}_{sm+1m_d}^{(t\mu)} (\mathcal{M}_{sm-1m_d}^{(t\mu)})^*, \quad (10)$$

where

$$\mathcal{Q} = \int_0^{q_{\max}} dq \iint d\Omega_{p_{NN}} \rho_s \sum_{smt} \sum_{m_\gamma m_d} \left| \mathcal{M}_{sm m_\gamma m_d}^{(t\mu)}(\vec{p}_{NN}, \vec{q}, \vec{k}) \right|^2. \quad (11)$$

(ii) The vector target asymmetry

$$\begin{aligned}T_{11} &= \frac{\sqrt{6}}{\mathcal{Q}} \mathcal{I}m \sum_{smt} \sum_{m_\gamma} \int_0^{q_{\max}} dq \iint d\Omega_{p_{NN}} \rho_s \left[ \mathcal{M}_{smt m_\gamma -1}^{(t\mu)} - \mathcal{M}_{smt m_\gamma +1}^{(t\mu)} \right] \\ &\times (\mathcal{M}_{smt m_\gamma 0}^{(t\mu)})^*.\end{aligned}\quad (12)$$

(iii) The tensor target asymmetries

$$T_{20} = \frac{1}{\sqrt{2}Q} \sum_{smt} \sum_{m_\gamma} \int_0^{q_{\max}} dq \iint d\Omega_{pNN} \rho_s \left[ |\mathcal{M}_{smm_\gamma+1}^{(t\mu)}|^2 + |\mathcal{M}_{smm_\gamma-1}^{(t\mu)}|^2 - 2 |\mathcal{M}_{smm_\gamma 0}^{(t\mu)}|^2 \right], \quad (13)$$

$$T_{21} = \frac{\sqrt{6}}{Q} \mathcal{R}e \sum_{smt} \sum_{m_\gamma} \int_0^{q_{\max}} dq \iint d\Omega_{pNN} \rho_s \left[ \mathcal{M}_{smm_\gamma-1}^{(t\mu)} - \mathcal{M}_{smm_\gamma+1}^{(t\mu)} \right] \times (\mathcal{M}_{smm_\gamma 0}^{(t\mu)})^*, \quad (14)$$

$$T_{22} = \frac{2\sqrt{3}}{Q} \mathcal{R}e \sum_{smt} \sum_{m_\gamma} \int_0^{q_{\max}} dq \iint d\Omega_{pNN} \rho_s \mathcal{M}_{smm_\gamma-1}^{(t\mu)} (\mathcal{M}_{smm_\gamma+1}^{(t\mu)})^*. \quad (15)$$

(iv) The longitudinal photon and deuteron double-polarization asymmetries

$$T_{20}^\ell = \frac{-1}{\sqrt{2}Q} \sum_{smt} \sum_{m_\gamma} \int_0^{q_{\max}} dq \iint d\Omega_{pNN} \rho_s \left[ (\mathcal{M}_{smm_\gamma-1}^{(t\mu)})^* \mathcal{M}_{s-mm_\gamma+1}^{(t\mu)} + (\mathcal{M}_{smm_\gamma+1}^{(t\mu)})^* \mathcal{M}_{s-mm_\gamma-1}^{(t\mu)} - 2 (\mathcal{M}_{smm_\gamma 0}^{(t\mu)})^* \mathcal{M}_{s-mm_\gamma 0}^{(t\mu)} \right], \quad (16)$$

$$T_{2\pm 2}^\ell = \frac{-\sqrt{3}}{Q} \sum_{smt} \sum_{m_\gamma} \int_0^{q_{\max}} dq \iint d\Omega_{pNN} \rho_s (\mathcal{M}_{smm_\gamma\pm 1}^{(t\mu)})^* \mathcal{M}_{s-mm_\gamma\pm 1}^{(t\mu)}. \quad (17)$$

As shown in our previous work [16,17], the asymmetries  $T_{10}^c$ ,  $T_{11}^c$ ,  $T_{20}^c$ ,  $T_{21}^c$ ,  $T_{22}^c$ ,  $T_{10}^\ell$ ,  $T_{1\pm 1}^\ell$  and  $T_{2\pm 1}^\ell$  vanish. Therefore, in what follows we shall discuss the results for only the  $\Sigma$ ,  $T_{11}$ ,  $T_{20}$ ,  $T_{21}$ ,  $T_{22}$ ,  $T_{20}^\ell$  and  $T_{2\pm 2}^\ell$  asymmetries.

## 5 Discussion of results

In this section we present our predictions of the polarization observables defined in Sect. 4 for the inclusive negative pion photoproduction reaction from the deuteron. For the elementary pion photoproduction operator on the free nucleon, the effective Lagrangian model developed by Schmidt *et al.* [8] has been considered. The two contributions to the pion production amplitude on the deuteron, i.e., the IA in (6) and the  $NN$ -rescattering in (7) are evaluated

by taking a realistic  $NN$  potential model for the deuteron wave function and the  $NN$  scattering amplitudes, in this work the Paris potential.

The discussion of the results is divided into three parts. First, we discuss the influence of  $NN$ -FSI on the single-polarization observables  $\Sigma$ ,  $T_{11}$ ,  $T_{20}$ ,  $T_{21}$ , and  $T_{22}$  by comparing the pure IA with the inclusion of  $NN$ -rescattering in the final state. In the second part, we consider the double-polarization asymmetries for photon and deuteron target. In the third one, we compare our results with the available experimental data. In all the plots that follow, the solid curves show the results of the full calculation, i.e., when  $NN$ -rescattering is included, while the dashed curves show the contribution of the pure IA alone in order to clarify the importance of  $NN$ -FSI effect.

### 5.1 *Single-spin asymmetries*

We begin the discussion by presenting our results for the single-spin asymmetries  $\Sigma$ ,  $T_{11}$ ,  $T_{20}$ ,  $T_{21}$ , and  $T_{22}$  in the pure IA and with  $NN$ -FSI, as shown in Figs. 2 through 11. The photon asymmetry  $\Sigma$  for linearly polarized photons at various photon lab-energies ( $\omega_\gamma = 200, 270, 330, 370, 420$  and  $500$  MeV) is plotted in Fig. 2 as a function of pion angle  $\theta_\pi$  in the lab frame. In order to show the sensitivity of the results to the photon lab-energy  $\omega_\gamma$ , we present in Fig. 3 the asymmetry  $\Sigma$  as a function of  $\omega_\gamma$  for fixed pion angles ( $\theta_\pi = 0^\circ, 90^\circ$  and  $180^\circ$ ). In the photon energy domain of the present work ( $\Delta(1232)$ -resonance region), the magnetic multipoles dominate over the electric ones, due to the excitation of the  $\Delta$ -resonance. This is clear from the dominantly negative values of  $\Sigma$  as shown in Fig. 2. We also see that the asymmetry  $\Sigma$  which is a ratio of cross sections is found to be sensitive to the energy of the incoming photon.

The left-top and right-bottom panels in Fig. 2 show that small positive values are found at  $\omega_\gamma = 200$  and  $500$  MeV. After including  $NN$ -FSI, we see that these positive values have disappeared at  $200$  MeV, while at  $500$  MeV these values are still evident at backward pion angles. At extreme forward and backward pion angles one can see, that the asymmetry  $\Sigma$  is relatively small in comparison to the results when  $\theta_\pi$  changes from about  $30^\circ$  to  $120^\circ$ . One also notices, that the contribution from  $NN$ -rescattering is much important in this region, in particular in the peak position. For lower and higher photon energies, one finds the strongest effect by  $NN$ -rescattering. It is also clear from Fig. 2 that the asymmetry  $\Sigma$  vanishes at  $\theta_\pi = 0^\circ$ , whereas a tiny negative value at  $180^\circ$  is observed.

We show in Fig. 4 the vector target asymmetry  $T_{11}$  as a function of pion angle in the lab frame for various photon lab-energies. The energy dependence of

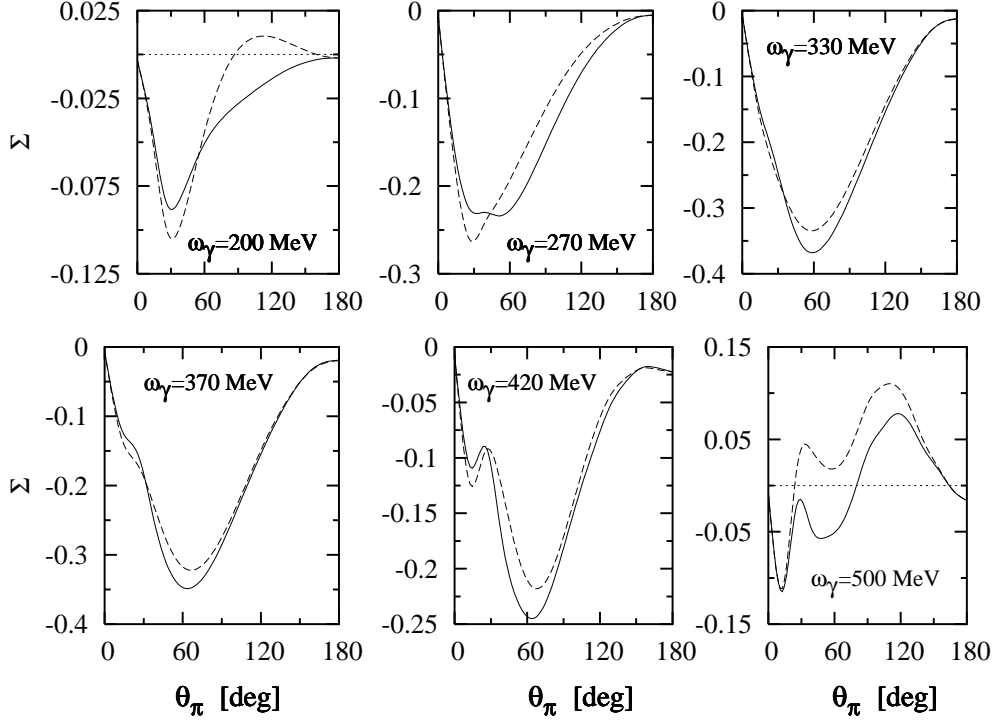


Figure 2. Linear photon asymmetry  $\Sigma$  for  $d(\vec{\gamma}, \pi^-)pp$  as a function of the emission pion angle  $\theta_\pi$  in the lab frame for various photon lab-energies  $\omega_\gamma$ . Notation of curves: dashed: IA; solid: IA+ $NN$ -rescattering.

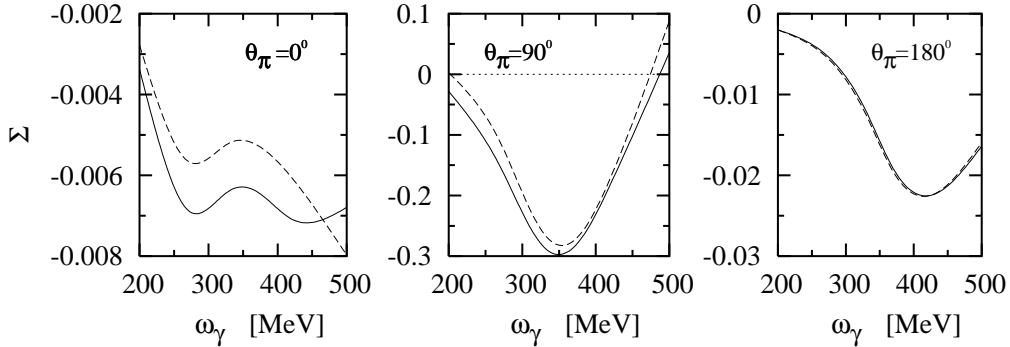


Figure 3. Linear photon asymmetry  $\Sigma$  for  $d(\vec{\gamma}, \pi^-)pp$  as a function of  $\omega_\gamma$  at fixed values of  $\theta_\pi$ . Notation as in Fig. 2.

this asymmetry for fixed pion angles is displayed in Fig. 5. In general, one can see that the  $T_{11}$  asymmetry has negative values even after including the  $NN$ -FSI. These values come mainly from the Born terms. It is also noticeable that the  $T_{11}$ -asymmetry vanishes at  $\theta_\pi = 0^\circ$  and  $180^\circ$  which is not the case for the linear photon asymmetry  $\Sigma$  as shown in Figs. 2 and 3. It is also apparent that the contribution of  $NN$ -FSI - the difference between the dashed and the solid curves - is very small, almost completely negligible at extreme forward and backward pion angles. Adding  $NN$ -FSI gives a slight increase (in absolute

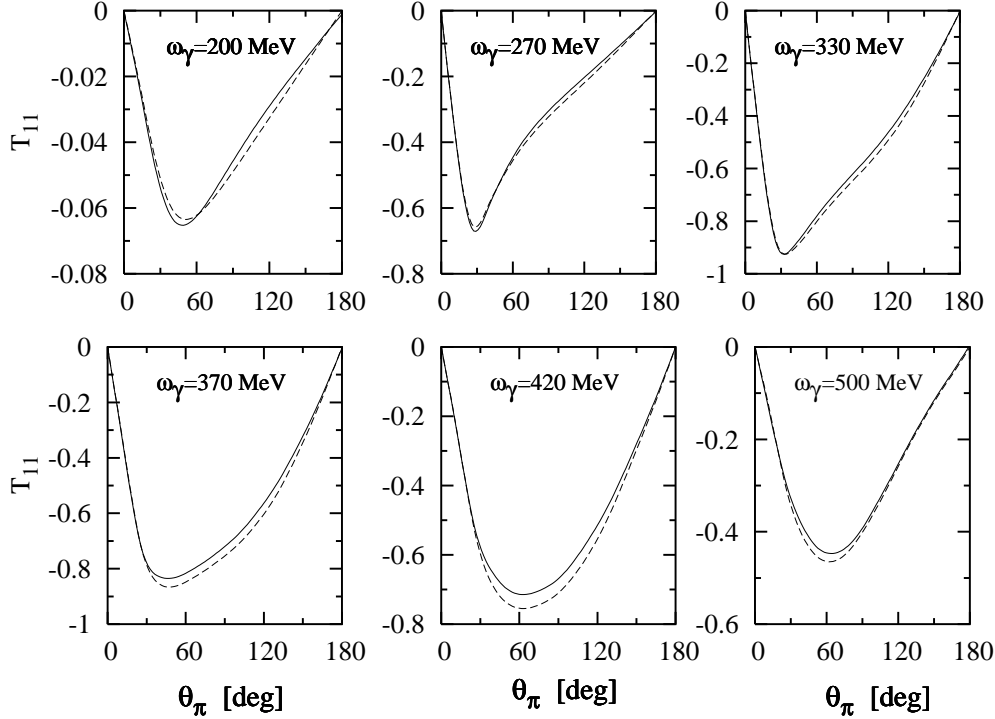


Figure 4. Vector target asymmetry  $T_{11}$  for  $\vec{d}(\gamma, \pi^-)pp$  as a function of  $\theta_\pi$  for various energies. Notation as in Fig. 2.

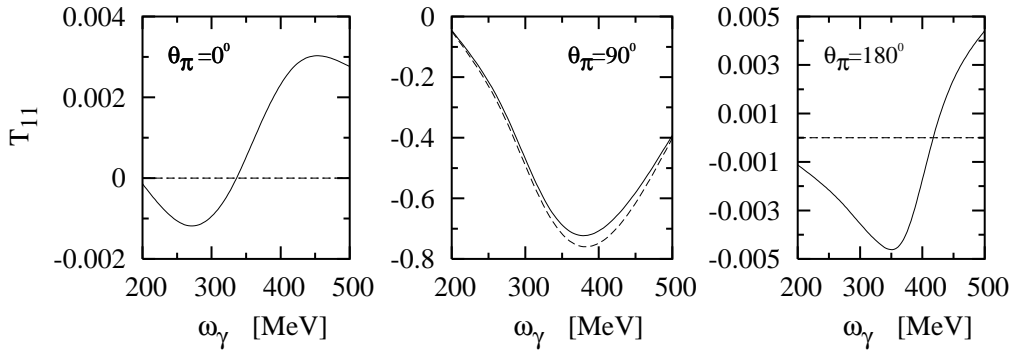


Figure 5. Vector target asymmetry  $T_{11}$  for  $\vec{d}(\gamma, \pi^-)pp$  as a function of  $\omega_\gamma$  at fixed values of  $\theta_\pi$ . Notation as in Fig. 2.

size decrease) of a few percent in the maximum.

Let us discuss now the results for the tensor target asymmetries  $T_{20}$ ,  $T_{21}$  and  $T_{22}$  as shown in Figs. 6 through 11. We emphasize that the tensor target asymmetries are found to be sensitive to the  $NN$ -FSI. In Figs. 6 and 7 we depict the results for the asymmetry  $T_{20}$  as a function of pion angle  $\theta_\pi$  for various energies (Fig. 6) and of photon lab-energy  $\omega_\gamma$  for fixed pion angles (Fig. 7). It is known [29] that the tensor target asymmetry  $T_{20}$  serves as a special tool to disentangle different reaction mechanisms. Comparing with the

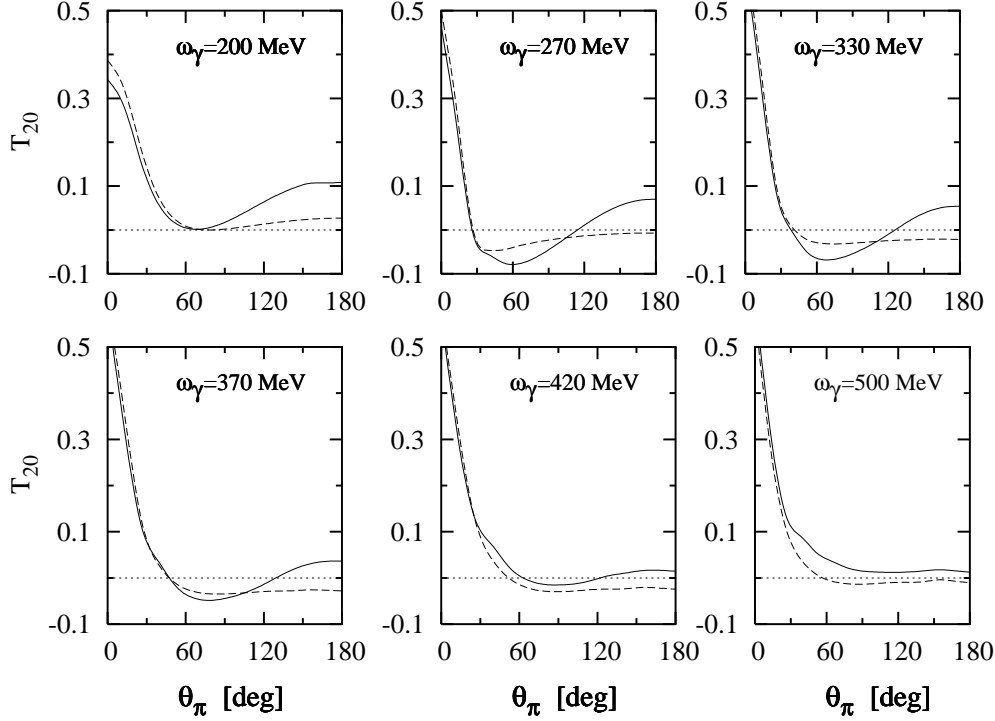


Figure 6. Tensor target asymmetry  $T_{20}$  for  $\vec{d}(\gamma, \pi^-)pp$  as a function of  $\theta_\pi$  for various energies. Notation as in Fig. 2.

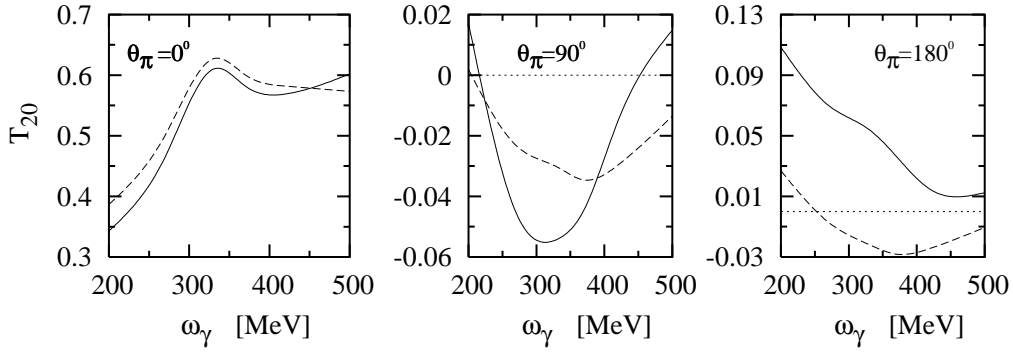


Figure 7. Tensor target asymmetry  $T_{20}$  for  $\vec{d}(\gamma, \pi^-)pp$  as a function of  $\omega_\gamma$  at fixed values of  $\theta_\pi$ . Notation as in Fig. 2.

results for linear photon and vector target asymmetries we found that the  $T_{20}$ -asymmetry has relatively large positive values at pion forward angles (at  $\theta_\pi < 30^\circ$ ) while small negative ones are found when  $\theta_\pi$  changes from  $30^\circ$  to  $180^\circ$ . Only at energies above the  $\Delta$ -region we observe small negative values at extreme backward angles. It is also obvious that the negative values appeared at extreme backward angles have totally disappeared after including the final-state  $NN$ -rescattering. Furthermore, quite a significant contribution from  $NN$ -FSI is found at pion backward angles. Intuitively, one would always expect that rescattering mechanisms become more important at higher

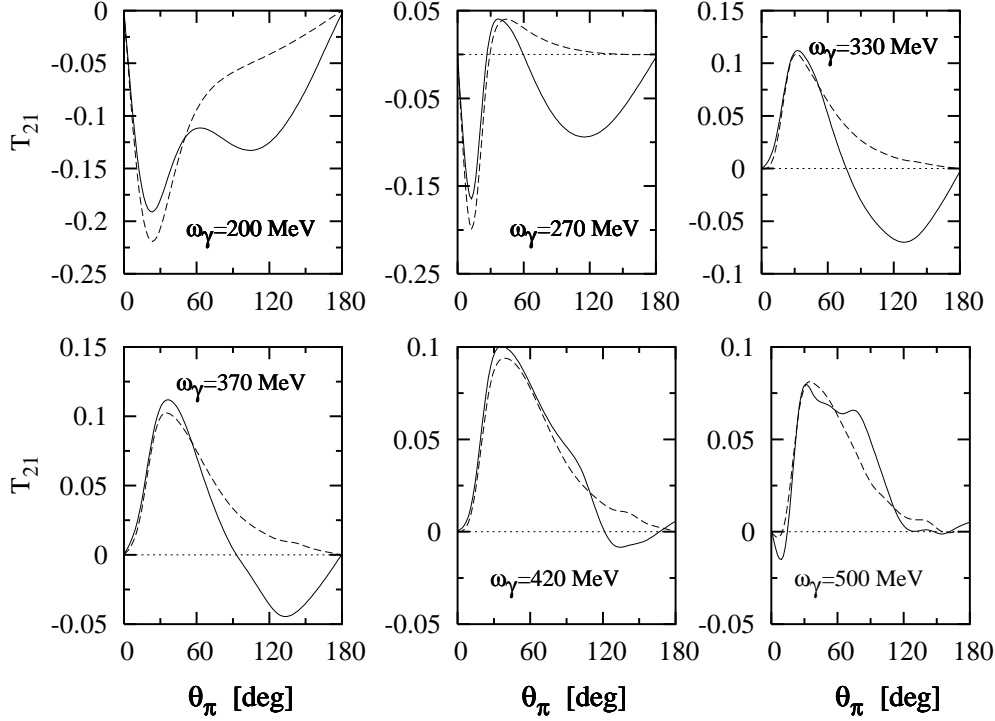


Figure 8. Tensor target asymmetry  $T_{21}$  for  $\vec{d}(\gamma, \pi^-)pp$  as a function of  $\theta_\pi$  for various energies. Notation as in Fig. 2.

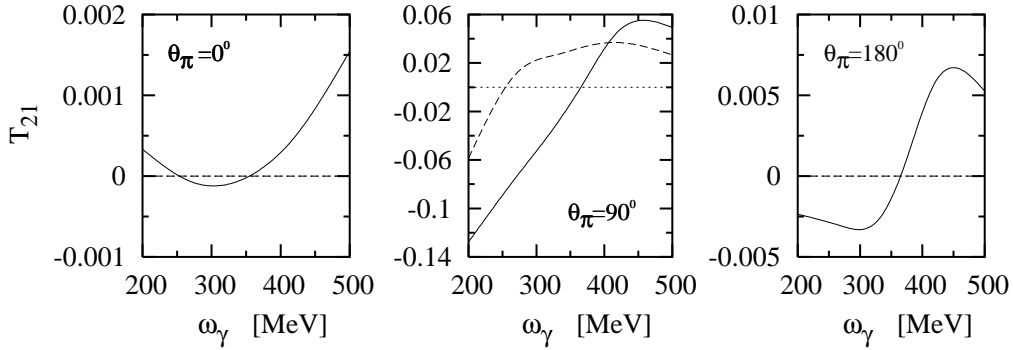


Figure 9. Tensor target asymmetry  $T_{21}$  for  $\vec{d}(\gamma, \pi^-)pp$  as a function of  $\omega_\gamma$  at fixed values of  $\theta_\pi$ . Notation as in Fig. 2.

momentum transfers, i.e., for larger scattering angles at fixed energy, since rescattering provides a means to share the momentum transfer between the two nucleons.

Predictions for the tensor target asymmetry  $T_{21}$  are shown in Figs. 8 (as a function of  $\theta_\pi$  for various  $\omega_\gamma$ ) and 9 (as a function of  $\omega_\gamma$  for fixed  $\theta_\pi$ ). It is clear that the  $T_{21}$  asymmetry has positive values at pion forward angles, which vanish at  $\theta_\pi = 180^\circ$ . At energies lower and higher than the  $\Delta(1232)$ -resonance region we see that  $T_{21}$  has negative values at extreme forward angles. Similar

to the case in the vector target asymmetry  $T_{11}$ , we found that the asymmetry  $T_{21}$  vanishes at  $\theta_\pi = 0^\circ$  and  $\theta_\pi = 180^\circ$ . One readily notes, that the  $NN$ -rescattering mechanism becomes much more effective at pion backward angles, in particular at  $\theta_\pi \simeq 120^\circ$ .

In Figs. 10 and 11 we present the results for the tensor target asymmetry  $T_{22}$  as a function of  $\theta_\pi$  for various  $\omega_\gamma$  (Fig. 10) and of  $\omega_\gamma$  for fixed  $\theta_\pi$  (Fig. 11). The same values of photon lab-energies as in the previous figures have been

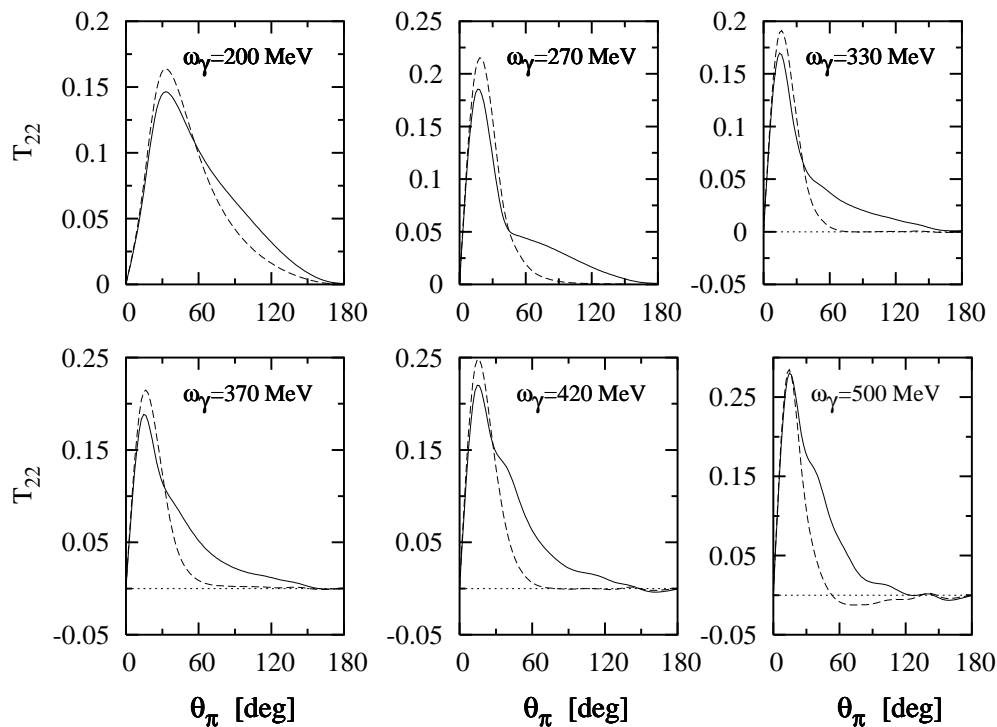


Figure 10. Tensor target asymmetry  $T_{22}$  for  $\vec{d}(\gamma, \pi^-)pp$  as a function of  $\theta_\pi$  for various energies. Notation as in Fig. 2.

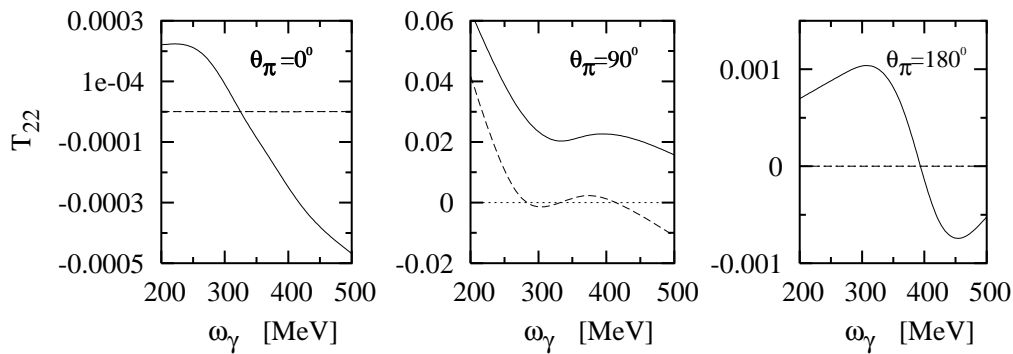


Figure 11. Tensor target asymmetry  $T_{22}$  for  $\vec{d}(\gamma, \pi^-)pp$  as a function of  $\omega_\gamma$  at fixed values of  $\theta_\pi$ . Notation as in Fig. 2.

used. Similar to the results of Figs. 6 through 9, one can see that the  $T_{22}$  asymmetry is sensitive to the values of pion angle  $\theta_\pi$  and photon energy  $\omega_\gamma$ . It is observed that, the asymmetry  $T_{22}$  has qualitatively large positive values at extreme forward angles. It is also obvious that  $T_{22}$  vanishes at  $\theta_\pi = 0^\circ$  and  $180^\circ$ .

From the foregoing discussion for the tensor target asymmetries it is apparent that the contribution of  $NN$ -FSI is important and must be considered in the analysis of the forthcoming experiments. This means, in particular with respect to a test of theoretical models for pion-production amplitudes on the neutron, that one needs a reliable description of the scattering process. Hopefully, these predictions can be tested in the near future when the data from the on-going experiments become available.

## 5.2 Beam-target double polarization asymmetries

As next we discuss the influence of  $NN$ -rescattering on beam-target double-polarization asymmetries as shown in Figs. 12 through 15. Interest in double-polarization observables comes from the recent technical improvements of electron accelerator facilities with both polarized beams and polarized targets. In view of these recent developments, it will soon be possible to measure double-spin observables with precision.

As already mentioned in section 4, the asymmetries  $T_{10}^c$ ,  $T_{11}^c$ ,  $T_{10}^\ell$ ,  $T_{1\pm 1}^\ell$ ,  $T_{20}^c$ ,  $T_{21}^c$ ,  $T_{22}^c$  and  $T_{2\pm 2}^\ell$  do vanish, whereas the spin asymmetries  $T_{20}^\ell$  and  $T_{2\pm 2}^\ell$  do not. Moreover, we would like to mention that the values for the  $T_{2\pm 2}^\ell$  asymmetry are found to be identical with the values of  $T_{2-2}^\ell$ . Therefore, in what follows we shall discuss the results for only the  $T_{20}^\ell$  and  $T_{2+2}^\ell$  asymmetries.

We show in Figs. 12 and 13 the influence of  $NN$ -rescattering on the longitudinal double-spin asymmetry  $T_{20}^\ell$  as a function of  $\theta_\pi$  for various energies (Fig. 12) and of  $\omega_\gamma$  for fixed angles (Fig. 13). We see that  $T_{20}^\ell$  has negative values at forward pion angles around  $\theta_\pi < 60^\circ$  which is not the case at backward pion angles. These negative values increase (in absolute value decrease) with increasing the photon energy. At extreme backward angles, we see that  $T_{20}^\ell$  has small positive values. We emphasize that the contribution from  $NN$ -FSI is much important in the energy region around the  $\Delta$ -resonance, especially in the peak position. One notices that the inclusion of  $NN$ -FSI leads to an overestimation by about 10% of the plane wave results. For lower and higher energies, one can see that the  $NN$ -FSI effect is small.

The predictions for the longitudinal double-polarization asymmetry  $T_{2+2}^\ell$  are plotted in Figs. 14 and 15 as a function of pion angle for various energies and of the photon lab-energy for fixed pion angles. The same values of photon lab-

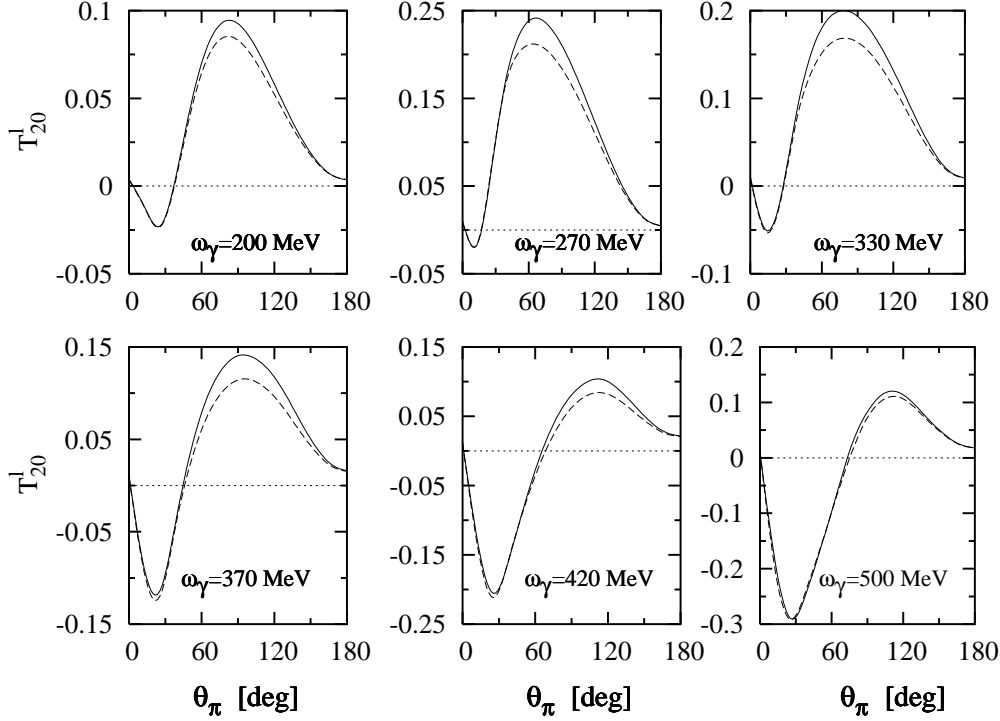


Figure 12. The double-polarization asymmetry  $T_{20}^\ell$  for  $\vec{d}(\vec{\gamma}, \pi^-)pp$  as a function of  $\theta_\pi$  for various energies. Notation as in Fig. 2.

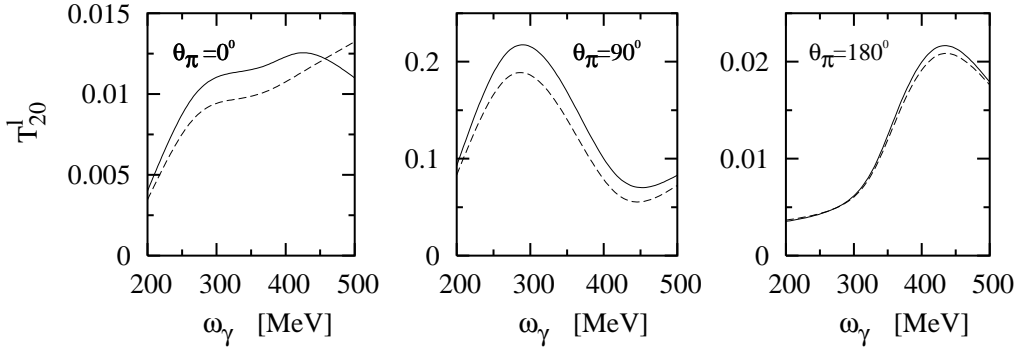


Figure 13. The double-polarization asymmetry  $T_{20}^\ell$  for  $\vec{d}(\vec{\gamma}, \pi^-)pp$  as a function of  $\omega_\gamma$  at fixed values of  $\theta_\pi$ . Notation as in Fig. 2.

energies and pion angles as the abovementioned cases are used. In general, one readily notices that the longitudinal asymmetry  $T_{2+2}^\ell$  has negative values even after including the contribution of  $NN$ -rescattering. Evidently, the values of  $T_{2+2}^\ell$  are sensitive to the photon energy and/or pion angle. We also emphasize that the  $NN$ -FSI shows rather insignificant effect.

We would like to mention that we have obtained essentially the same results for the foregoing polarization asymmetries if we take the Bonn r-space potential model instead of the Paris one to estimate the half-off-shell partial wave  $NN$

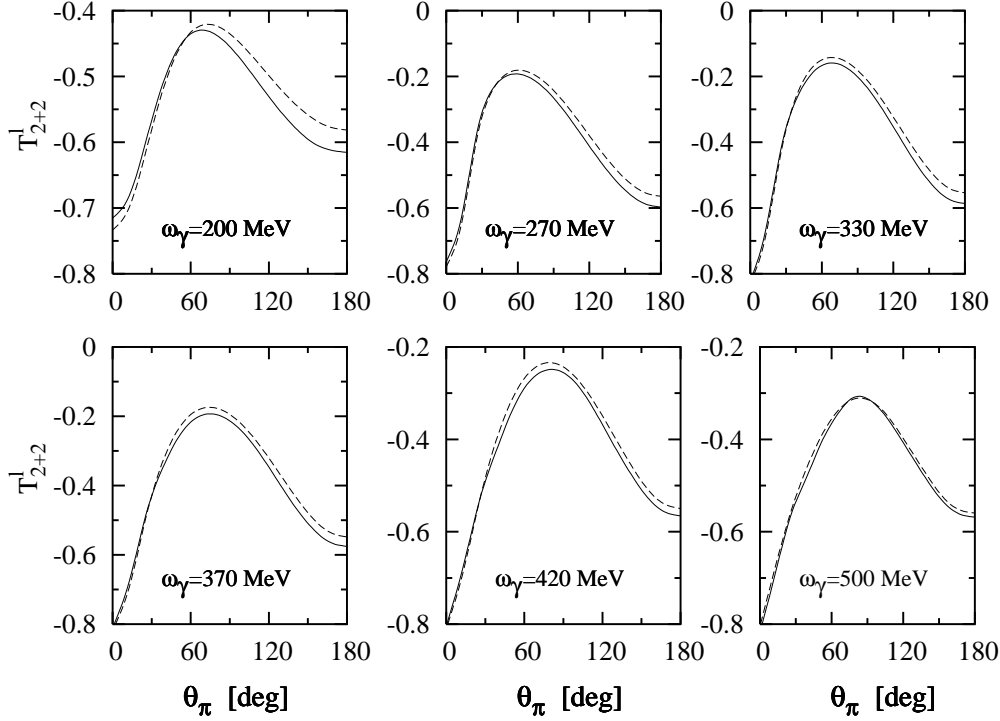


Figure 14. The double-polarization asymmetry  $T_{2+2}^\ell$  for  $\vec{d}(\vec{\gamma}, \pi^-)pp$  as a function of  $\theta_\pi$  for various energies. Notation as in Fig. 2.

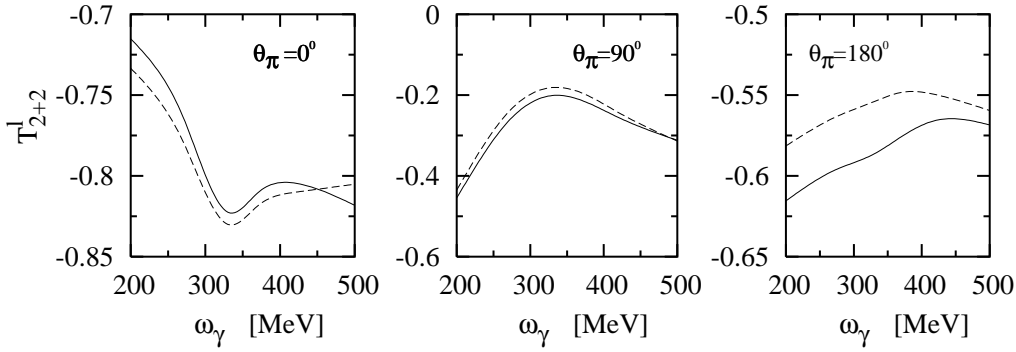


Figure 15. The double-polarization asymmetry  $T_{2+2}^\ell$  for  $\vec{d}(\vec{\gamma}, \pi^-)pp$  as a function of  $\omega_\gamma$  at fixed values of  $\theta_\pi$ . Notation as in Fig. 2.

amplitudes in (8).

### 5.3 Comparison with experimental data

Here we compare our results with the available experimental data. Most recently, a few preliminary data points are available from the LEGS Spin collaboration [19] for the linear photon asymmetry  $\Sigma$ , but with regard to the

other polarization observables, there are no data whatsoever. In Fig. 16 we confront these experimental data with our theoretical results in the pure IA (dashed curves) and with  $NN$ -rescattering (solid curves) at two photon lab-energies  $\omega_\gamma = 270$  and 330 MeV in order to establish the present status of our knowledge of this important asymmetry. We see that the general feature of the data is reproduced. However, the discrepancy is rather significant in the region where the photon energy close to the  $\Delta$ -resonance. This could be due to the higher order rescattering mechanisms which are neglected in this work. It is obvious, therefore, that for a conclusive interpretation, one has to include all corrections of FSI and two-body effects consistently. In the same figure, we also show the results from the IA only (dashed curves). It is seen that the  $NN$ -rescattering yields an about 10% effect in the region of the peak position. We found that this is mainly due to the interference between the IA amplitude and the  $NN$ -FSI amplitude.

In agreement with our previous results [17], one notes that the pure IA (dashed curves in Fig. 16) cannot describe the experimental data. The inclusion of  $NN$ -FSI leads at  $\omega_\gamma = 270$  MeV to a quite satisfactory description of the data, whereas at 330 MeV  $NN$ -FSI effect is small and therefore differences between theory and experiment are still evident. An experimental check of the  $\Sigma$ -asymmetry covering a large range for the emission pion angle and the photon lab-energy would provide an additional significant test of our present theoretical understanding of this spin observable.

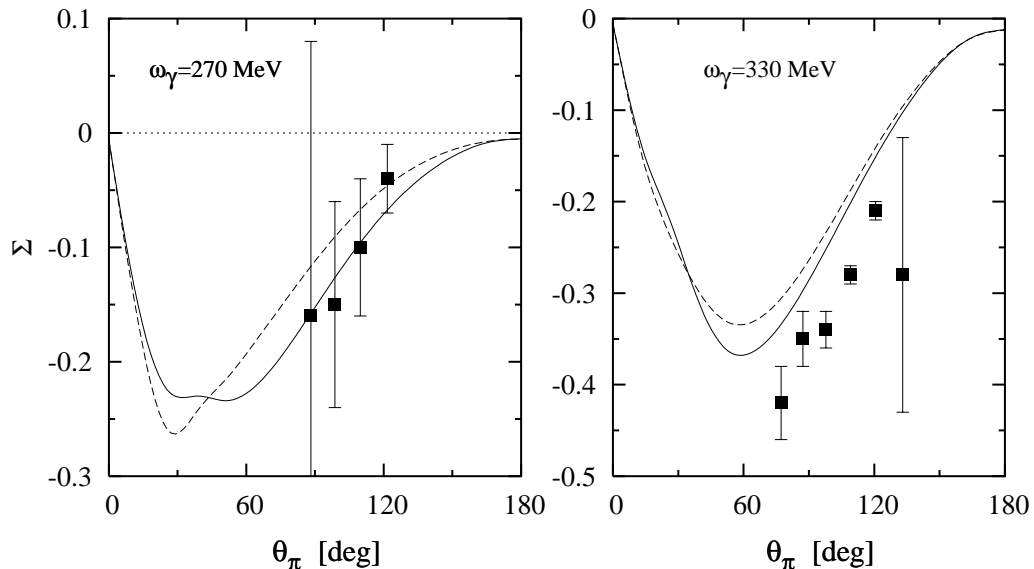


Figure 16. Linear photon asymmetry  $\Sigma$  for the reaction  $d(\vec{\gamma}, \pi^-)pp$  as a function of  $\theta_\pi$  at  $\omega_\gamma = 270$  and 330 MeV in comparison with the preliminary data from LEGS [19]. Notation as in Fig. 2.

## 6 Conclusions

In the present paper, we have presented calculations for polarization observables in incoherent negative pion photoproduction from the deuteron in the  $\Delta(1232)$ -resonance region taking into account the  $NN$ -rescattering in the final state. The influence of  $NN$ -FSI on various single- and double-spin observables is investigated. In view of the results presented in this paper, one has to conclude that the contribution of  $NN$ -rescattering effect must be taken into account in the analysis of experimental data for spin observables. Compared to the preliminary experimental data for the linear photon asymmetry [19], one notices a remaining discrepancy even if  $NN$ -FSI is included. Therefore, further investigations are required. Specifically, it will be interesting to see whether this remaining discrepancy is connected with a complete three-body treatment of the final  $\pi NN$  system.

Concluding this paper, we would like to mention, that the forthcoming experimental data on spin-dependent observables are very welcome since it is expected that they might play an important role in deepening our theoretical understanding of the incoherent pion photoproduction reaction from the deuteron. On the theoretical side, we have to improve the treatment by including higher order rescattering and two-body effects in order to obtain a more realistic description of these important spin observables. Furthermore, an independent calculations in the framework of effective field theory would be very interesting.

## Acknowledgements

This work is supported in part by the Bibliotheca Alexandrina - Center for Special Studies and Programs - under grant number: 2602314 Sohag 2<sup>nd</sup>-Sohag. We are indebted to Profs. H. Arenhövel, T.-S. Harry Lee, T. Sato and A. Sandorfi for fruitful discussions and valuable informations.

## References

- [1] V. Burkert, T.-S. H. Lee, Int. J. Mod. Phys. E 13 (2004) 1035.
- [2] B. Krusche, S. Schadmand, Prog. Part. Nucl. Phys. 51 (2003) 399.
- [3] G.F. Chew, H.W. Lewis, Phys. Rev. 84 (1951) 779.
- [4] M. Lax, H. Feshbach, Phys. Rev. 88 (1952) 509.

- [5] I. Blomqvist, J.M. Laget, Nucl. Phys. A 280 (1977) 405.
- [6] J.M. Laget, Nucl. Phys. A 296 (1978) 388.
- [7] J.M. Laget, Phys. Rep. 69 (1981) 1.
- [8] R. Schmidt, H. Arenhövel, P. Wilhelm, Z. Phys. A 355 (1996) 421.
- [9] M.I. Levchuk, M. Schumacher, F. Wissmann, nucl-th/0011041.
- [10] E.M. Darwish, H. Arenhövel, M. Schwamb, Eur. Phys. J. A 16 (2003) 111.
- [11] I.T. Obukhovskiy *et al.*, J. Phys. G: Nucl. Part. Phys. G 29 (2003) 2207.
- [12] A.Yu. Loginov, A.A. Sidorov, V.N. Stibunov, Phys. Atom. Nucl. 63 (2000) 391.
- [13] A.Yu. Loginov, A.V. Osipov, A.A. Sidorov, V.N. Stibunov, nucl-th/0407045.
- [14] E.M. Darwish, H. Arenhövel, M. Schwamb, Eur. Phys. J. A 17 (2003) 513.
- [15] E.M. Darwish, Nucl. Phys. A 735 (2004) 200.
- [16] E.M. Darwish, Int. J. Mod. Phys. E 13 (2004) 1191.
- [17] E.M. Darwish, J. Phys. G: Nucl. Part. Phys. G 31 (2005) 105.
- [18] E.M. Darwish, Phys. Lett. B (2005) (in press).
- [19] A. Sandorfi, M. Lucas, private communication;  
M. Lucas, in LQWq Workshop on Electromagnetic Nucleon Reactions at Low Momentum Transfer, 23-25 August, 2001, Halifax, Nova Scotia, Canada.
- [20] E.M. Darwish, Nucl. Phys. A 748 (2005) 596.
- [21] E.M. Darwish, Prog. Theor. Phys. 113 (2005) 169.
- [22] P. Pedroni, private communication;  
C.A. Rovelli, Diploma Thesis, University of Pavia, Italy, 2002.
- [23] J. Haidenbauer, W. Plessas, Phys. Rev. C 30 (1984) 1822;  
J. Haidenbauer, W. Plessas, Phys. Rev. C 32 (1985) 1424.
- [24] D.J. Ernst, C.M. Shakin, R.M. Thaler, Phys. Rev. C 8 (1973) 46;  
D.J. Ernst, C.M. Shakin, R.M. Thaler, Phys. Rev. C 9 (1974) 1780.
- [25] M. Lacombe *et al.*, Phys. Rev. C 21 (1980) 861.
- [26] H. Garcilazo, T. Mizutani,  $\pi NN$  Systems, World Scientific, Singapore, 1990.
- [27] J.D. Bjorken, S.D. Drell, Relativistic Quantum Mechanics, McGraw-Hill, New York, 1964.
- [28] H. Arenhövel, Few-Body Systems 4 (1988) 55.
- [29] P. Wilhelm, H. Arenhövel, Nucl. Phys. A 609 (1996) 469.